

NEURAL: quantitative features for newborn EEG using Matlab

John M. O' Toole^{a,*}, Geraldine B. Boylan^a

^aNeonatal Brain Research Group, Irish Centre for Fetal and Neonatal Translational Research (INFANT), University College Cork, Ireland

Abstract

Background: For newborn infants in critical care, continuous monitoring of brain function can help identify infants at-risk of brain injury. Quantitative features allow a consistent and reproducible approach to EEG analysis, but only when all implementation aspects are clearly defined. *Methods:* We detail quantitative features frequently used in neonatal EEG analysis and present a Matlab software package together with exact implementation details for all features. The feature set includes stationary features that capture amplitude and frequency characteristics and features of inter-hemispheric connectivity. The software, a Neonatal Eeg featURe set in mAtLab (NEURAL), is open source and freely available. The software also includes a pre-processing stage with a basic artefact removal procedure. *Conclusions:* NEURAL provides a common platform for quantitative analysis of neonatal EEG. This will support reproducible research and enable comparisons across independent studies. These features present summary measures of the EEG that can also be used in automated methods to determine brain development and health of the newborn in critical care.

Keywords: neonate, preterm infant, electroencephalogram, quantitative analysis, feature extraction, spectral analysis, inter-burst interval

Abbreviations: EEG, electroencephalogram; NEURAL, neonatal EEG feature set in MATLAB; NICU, neonatal intensive care unit; aEEG, amplitude-integrated EEG; rEEG, range EEG; PSD, power spectral density; BSI, brain symmetry index; FIR, finite impulse response; IIR, infinite impulse response; DFT, discrete Fourier transform; CC, correlation coefficient.

1. Introduction

Electroencephalography (EEG) is used in the neonatal intensive care environment to monitor brain function of critically-ill newborns. This non-invasive and portable technology provides continuous assessment of cortical function at the cot side, with little interruption to standard clinical care. Specialists are required to visually interpret the EEG to evaluate brain health, by identifying seizures if present [1], assessing brain maturation [2], or grading brain injury [3]. Yet in many neonatal intensive care units (NICUs), provision for continuous reporting on the EEG of multiple infants is constrained by the availability of the specialist. Addressing this limitation, many NICUs use an amplitude-integrated EEG (aEEG) device instead of the EEG. The aEEG presents a band-pass filtered and time-compressed version of 1 or 2 channels of EEG [4, 5]. Because of the time-compression, a long duration EEG (approximately 6 hours) is summarised in 1 page, making reviewing an easier task that is often preformed by non-EEG specialists, such as the treating clinician. Yet the time-compression destroys much of the detail of the EEG waveform and many important clinical features, such as short-duration seizures, are not presented on the aEEG [4]. In addition, artefacts can falsely enhance baseline activity or may be misinterpreted as seizures [6–8].

*Corresponding author

Email addresses: jotoole@ucc.ie (John M. O' Toole), G.Boylan@ucc.ie (Geraldine B. Boylan)

Quantitative EEG analysis provides an alternative to visual interpretation, with specific advantages. First, quantitative analysis provides consistency without the varying degrees of inter-rater agreement associated with visual interpretation [9]. Second, quantitative analysis can uncover attributes not accessible with visual analysis alone, such as measures of connectivity [10, 11]. Third, quantitative analysis can facilitate reproducible research for clinical, scientific, and engineering studies. And last, quantitative analysis is a necessary component for developing fully automated methods of EEG analysis [12–14]. This is of particular importance as automated analysis of the EEG addresses the need to provide continuous, around-the-clock EEG reporting in the NICU—something not possible with visual interpretation alone.

Quantitative features describe many aspects of newborn EEG, including sleep cycles [15–18], normative ranges [19–25], association with clinical outcomes [26–30], and functional maturation [14, 31–36]. Not strictly defined, the term *quantitative EEG features* typically refers to basic signal processing measures of frequency and amplitude. Most measures assume the signal is stationary and therefore rely on short-time analysis to circumvent this assumption. Although the features frequently appear in EEG literature, implementation details are often omitted which makes comparison between independent studies difficult, as different implementations will generate different estimates. The goal of this paper, therefore, is to present a clearly defined feature set with a software implementation that is both open source and freely available. We hope the availability of this feature set will enhance comparisons between different studies, support reproducible research, and enhance quantitative analysis of neonatal EEG.

2. NEURAL: software package for Matlab

The software package *NEURAL*—a neonatal EEG feature set in `matlab` (v0.3.1)—runs within the MATLAB environment (The MathWorks, Inc., Natick, Massachusetts, United States). Details on how to install and setup the MATLAB code is described in the `README.md` file accompanying the package [37]. The package can generate multiple features on continuous, multi-channel EEG recordings. Features are defined specifically for neonatal EEG, including preterm infants, but could also be applied to paediatric and adult EEG.

Features are grouped into 4 categories:

- **amplitude**: absolute amplitude and envelope of EEG signal, range EEG (similar to amplitude-integrated EEG); full list in Table B.1.
- **spectral**: spectral power (absolute and relative), spectral entropy (Wiener and Shannon), spectral differences, spectral edge frequency, and fractal dimension; full list in Table B.2.
- **connectivity**: coherence, cross-correlation, and brain symmetry index; full list in Table B.3.
- **inter-burst interval**: summary measures based on the inter-burst interval annotation (only relevant to preterm infants <32 weeks of gestational age); full list in Table B.4.

All features are listed in Tables B.2–B.4 and in file `all_features_list.m`. Parameters, for both the features and pre-processing stage, are set in the `neural_parameters.m` file. For example, the low-pass filter and new sampling frequency are set in `neural_parameters.m` as

```
1 %% PREPROCESSING (lowpass filter and resample)
2 LP_fc=30; % low-pass filter cut-off
3 Fs_new=64; % down-sample to Fs_new (Hz)
```

Default values set in this file are reported throughout.

Unless otherwise stated, we use infinite impulse response (IIR) filters for all band-pass filtering operations, for both the artefact removal and feature estimation procedures. These filters are generated with a 5th order Butterworth design and implemented using the forward-backwards approach to generate a zero-phase response [38].

3. Pre-processing: Artefact Removal

If required, the raw EEG can be pre-processed and then saved as Matlab files. Pre-processing includes a simple artefact removal procedure followed by low-pass filtering and downsampling. The function

`resample_savemat.m` performs the pre-processing. The artefact removal process removes major artefacts only, such as electrode coupling or large-amplitude segments caused by movement; this process is detailed in the following and includes similar procedures to those described in [14]. If the EEG is still contaminated by other artefacts, such as respiration and heart rate, other methods may also be needed [39]. After artefact removal, all EEG channels are low-pass filtered (with a default frequency of 30 Hz; parameter `LP_fc`) using a finite-impulse response (FIR) filter. This filter is designed using the window method with a Hamming window of length 4,001 samples. The EEG is then downsampled to a lower frequency (default 64 Hz; parameter `Fs_new`).

To enable the artefact removal process, set `REMOVE_ART=1` if using function `resample_savemat.m`; otherwise, to turn off set `REMOVE_ART=0`. The process can also be implemented directly using the `remove_artefacts.m` function—see Section 5.1 for an example on how to use this function. The following details 5 stages of the artefact removal process. The process requires both the bipolar (set with `BI_MONT`) and referential montage of EEG.

The first stage is applied to the $(M + 1)$ -channel referential montage. Each channel $x_m[n]$, for $m = 1, 2, \dots, M, M + 1$, is length- N .

1. Improper electrode placement:

- (a) filter each channel $x_m[n]$ with 0.5–20 Hz bandpass filter;
- (b) generate correlate coefficient r_{pq} between channel p and q , for $p, q = 1, 2, \dots, M$, with $p \neq q$;
- (c) average r_{pq} over q , that is let $\bar{r}_p = 1/(M - 1) \sum_{q=1; q \neq p}^{M-1} r_{pq}$ for all p ;
- (d) for $\bar{r}_p < T_{cc}$ then remove channel p from further analysis (default $T_{cc} = 0.15$; parameter `ART_REF_LOW_CORR`)

The next stage uses the M channel bipolar montage, with $x_m[n]$ now representing each bipolar channel.

2. Electrode coupling:

- (a) filter each channel $x_m[n]$ with 0.5–20 Hz bandpass filter;
- (b) generate total power for the m th channel $P_m = 1/N \sum_{n=0}^{N-1} |x_m[n]|^2$;
- (c) let l denote the index of left-hemisphere channels only, where $\{l\}$ is a length- $M/2$ subset of $\{m\}$;
- (d) let $T_{\text{left}} = \text{median}(P_l)/4$
- (e) if $P_l < T_{\text{left}}$, remove l th channel;
- (f) repeat previous 3 steps for right-hemisphere channels.

For the remaining stages process each bipolar channel $x[n]$ separately.

3. Continuous rows of zeros (on some EEG devices zeros replace EEG when testing for electrode impedance):

- (a) identify segments $x[n] = 0$ for $n = n + 1, n + 2, \dots, n + L$;
- (b) if $L > T_{\text{min.dur}}$, then remove (default $T_{\text{min.dur}} = 1$ second; parameter `ART_ELEC_CHECK`).

4. High-amplitude artefacts:

- (a) filter $x[n]$ with a [0.1–40] Hz bandpass filter;
- (b) generate the analytic associate of $x[n]$ as $z[n] = x[n] + j\mathcal{H}\{x[n]\}$, using the Hilbert transform \mathcal{H} .
- (c) if $|z[n]| > T_{\text{amp}}$, then remove this segment (default $T_{\text{amp}} = 1500\mu V$, suitable for preterm infants <32 weeks of gestation; parameter `ART_HIGH_VOLT`)
- (d) apply a collar around this segment and remove; default collar length is 10 seconds (parameter `ART_TIME_COLLAR`).

5. Row of constant values or impulse-like activity (sudden jumps in amplitude):

- (a) calculate the derivative of $x[n]$ using the forward-difference approximation $x'[n] = x[n + 1] - x[n]$;
- (b) identify $x'[n] = C$ for $n = n + 1, n + 2, \dots, n + L$, where C is a constant;
- (c) if $L > T_{\text{min.dur}}$, then remove (default $T_{\text{min.dur}} = 0.1$ seconds; parameter `ART_DIFF_MIN_TIME`);
- (d) if $|x'[n]| > T_{\text{amp.diff}}$, then remove (default $T_{\text{amp.diff}} = 200\mu V$; parameter `ART_DIFF_VOLT`).
- (e) apply a collar around both artefacts if present and remove; default length of collar is 0.5 seconds (parameter `ART_DIFF_TIME_COLLAR`)

For artefacts identified on a single channel (preceding stages 3–5), the same segments are removed over all channels. Identified artefacts are replaced by either zeros, linear interpolation, or cubic spline interpolation;

default is cubic spline interpolation, parameter `FILTER_REPLACE_ARTEFACTS='cubic_interp'`. For stages 1–2, if channels are identified as artefacts they are then removed from further analysis.

4. Features

All features are estimated using the bipolar montage of the EEG. Many features are estimated within four different frequency bands of the EEG. Default values for these bands are [0.5–4; 4–7; 7–13; 13–30] Hz, recommended for infants ≥ 32 weeks, or [0.5–3; 3–8; 8–15; 15–30] Hz for preterm infants < 32 weeks of gestation [14]. These bands are set with the `FREQ_BANDS` parameter and can also be set individually for the specific feature, as we describe in the following.

4.1. Amplitude

Each EEG channel $x[n]$ is filtered into the four frequency bands to generate $x_i[n]$ ($i = 1, 2, 3, 4$). These bands can be set with the parameter `feat_params_st.amplitude.freq_bands`. Amplitude is quantified by signal power and signal envelope. Signal power (A_{power}^i) is calculated as the mean value, over time (n), of $|x_i[n]|^2$ and amplitude of signal envelope (E_{mean}^i) is calculated as the mean value of envelope $e_i[n]$, with

$$e_i[n] = |x_i[n] + j\mathcal{H}\{x_i[n]\}|^2 \quad (1)$$

where \mathcal{H} represents the discrete Hilbert transform implemented according to the definition described by Marple [40].

Measures of variability of the EEG about a mean value are estimated by the standard deviation (A_{sd}^i) of $x_i[n]$ and standard deviation of the envelope $e_i[n]$. Skewness and kurtosis (A_{sk}^i and A_{ks}^i) of $x_i[n]$ are calculated to estimate a non-Gaussian processes. Moments of the probability distribution (mean, standard deviation, skew, and kurtosis) are defined in [Appendix A](#).

Also included are features of the range-EEG (rEEG) [33]. rEEG was proposed as an alternative to amplitude-integrated EEG (aEEG) as there is no clear definition of aEEG in the literature and most EEG machines implement different versions of the aEEG algorithm [41]. Although another measure of amplitude, the rEEG estimates a peak-to-peak measure of voltage and therefore differs to the previous measures.

We can calculate features of rEEG using either the full-band signal $x[n]$ or on the individual frequency bands $x_i[n]$, which gives more flexibility than aEEG which uses a fixed pass-band of 2–15 Hz [4, 41]. (The passband 2–15 Hz is suboptimal for neonatal EEG analysis given the predominance of delta power in neonatal EEG.) Over a short-time windowed segment, the difference between the maximum and minimum is generated

$$r_i[l] = \max(x_i[n]w[n - lK]) - \min(x_i[n]w[n - lK]) \quad (2)$$

for window $w[n]$ (default rectangular window of length 2 seconds, parameters `feat_params_st.rEEG.window_type` and `feat_params_st.rEEG.L_window`) and time-shift factor K (parameter `feat_params_st.rEEG.overlap`) related to the percentage overlap H and window length M as $K = \lceil M(1 - H/100) \rceil$. When plotting, the rEEG is transformed to a linear–log amplitude as follows

$$r_i[l] = \begin{cases} \frac{50}{\log 50} \log r_i[l] & \text{if } r_i[l] > 50 \\ r_i[l] & \text{otherwise} \end{cases} \quad (3)$$

Multiple features are used to summarise $r_i[l]$: mean (R_{mean}^i) and median (R_{median}^i) as measures of central tendency; the 5th (R_{lower}^i) and 95th (R_{upper}^i) percentiles to represent the lower and upper margins; standard deviation (R_{sd}^i), the coefficient of variation ($R_{\text{cv}}^i = R_{\text{sd}}^i/R_{\text{mean}}^i$), the difference between the upper and lower margins ($R_{\text{bw}}^i = R_{\text{upper}}^i - R_{\text{lower}}^i$) as measures of spread, and a measure of symmetry defined as

$$R_{\text{symm}}^i = \frac{(R_{\text{upper}}^i - R_{\text{median}}^i) - (R_{\text{median}}^i - R_{\text{lower}}^i)}{R_{\text{bw}}^i} \quad (4)$$

where R_{symm}^i ranges from -1 to 1 with values close to 0 indicating symmetry and values close to ± 1 indicating asymmetry of the rEEG.

4.2. Frequency

The following measures quantify spectral characteristics. First we present 3 ways to estimate the power spectral density (PSD) for EEG signal $x[n]$ of length- N with sampling frequency f_s Hz. These different PSD estimates are used in different features. The first PSD estimate is the periodogram $V[k]$ using a rectangular window

$$V[k] = \frac{1}{Nf_s} \left| \sum_{n=0}^{N-1} x[n]e^{-j2\pi kn/N} \right|^2. \quad (5)$$

The second PSD estimate is the Welch periodogram $P[k]$

$$P[k] = \frac{1}{LMUf_s} \sum_{l=0}^{L-1} \left| \sum_{n=0}^{M-1} x[n]w[n-lK]e^{-j2\pi kn/M} \right|^2 \quad (6)$$

where $w[n]$ is the analysis window of length M with energy $U = 1/M \sum_{n=0}^{M-1} |w[n]|^2$; default settings apply a Hamming window of length 2 seconds, set with parameters `feat_params_st.spectral.window_type` and `feat_params_st.spectral.L_window`. The time-shift factor K is related to the percentage overlap H and window length M , as $K = \lceil M(1 - H/100) \rceil$. Lastly, $L = \lfloor (N + K - M)/K \rfloor$ is the number of segments. Default value for H is 50%, set with parameter `feat_params_st.spectral.overlap`. And the third PSD estimate is a variant of the Welch periodogram, defined as

$$P_{\text{med}}[k] = \text{median}_{l \in [0, L-1]} \left\{ \frac{1}{MUf_s} \left| \sum_{n=0}^{M-1} x[n]w[n-lK]e^{-j2\pi kn/M} \right|^2 \right\} \quad (7)$$

This estimate, which we refer to as the robust-PSD estimate, simply replaces the averaging procedure of the Welch periodogram in (6) with the median operator to generate a more robust spectral estimate [42].

For features of absolute and relative spectral power at the i th frequency band, we use the periodogram $V[k]$ in (5):

$$S_{\text{abspow}}^i = \frac{s[k]f_s}{N} \sum_{k=a_i}^{b_i} V[k] \quad (8)$$

$$S_{\text{relpow}}^i = \frac{\sum_{k=a_i}^{b_i} V[k]}{\sum_{k=a_1}^{b_4} V[k]} \quad (9)$$

where $[a_i, b_i]$ represents the discrete frequency range of the i th frequency band. The parameter $s[k]$ is a scaling factor, with $s[k] = 2$ for $k = 1, 2, \dots, \lceil N/2 \rceil - 1$ and $s[k] = 1$ for the DC ($k = 0$) and Nyquist frequency ($k = N/2$, for N even only). This scaling factor is applied to conserve total power in the spectrum when using only the positive frequencies of $V[k]$.

Spectral entropy measures are estimated using Wiener entropy, also known as *spectral flatness*, and Shannon entropy:

$$F_{\text{wiener}}^i = \frac{\exp\left(1/L_i \sum_{k=a_i}^{b_i} \log P[k]\right)}{1/L_i \sum_{k=a_i}^{b_i} P[k]} \quad (10)$$

$$F_{\text{shannon}}^i = -\frac{1}{\log L_i} \sum_{k=a_i}^{b_i} \bar{P}_i[k] \log \bar{P}_i[k] \quad (11)$$

where L_i is the length of sequence $[a_i, b_i]$ representing the range of the frequency band. The normalised spectral density $\bar{P}_i[k]$ is calculated as $\bar{P}_i[k] = P[k] / \sum_{k=a_i}^{b_i} P[k]$. For these two entropy features, the PSD estimate $P[k]$ is either the periodogram in (5), the Welch periodogram in (6), or the robust estimate in (7).

This option is set with the parameter `feat_params_st.spectral.method` as either `'periodogram'`, `'PSD'` (the default), or `'robust-PSD'`.

Spectral edge frequency is defined as the frequency f_{SEF} that contains $d\%$ (default 95%, parameter `feat_params_st.spectral.SEf`) of the spectral energy; that is, we find f_{SEF} that satisfies the relation

$$\frac{d}{100} = \frac{\sum_{k=a_1}^{f_{\text{SEF}}} P[k]}{\sum_{k=a_1}^{b_4} P[k]}. \quad (12)$$

As for the spectral entropy measures, the PSD estimate $P[k]$ can be either one of the 3 estimates in (5), (6), and (7), set with the parameter `feat_params_st.spectral.method`.

Spectral difference is measured as the difference between consecutive time-slices of the spectrogram (a time-varying spectral estimate). The spectrogram, with window $w[n]$, is defined as

$$S[n, k] = \left| \sum_{m=0}^{N-1} x[m]w[m-n]e^{-j2\pi km/N} \right|^2 \quad (13)$$

and the difference is calculated as

$$F_{\text{specdiff}} = \text{median} \left\{ \frac{1}{L_i} \sum_{k=a_i}^{b_i} |\bar{S}^i[n, k] - \bar{S}^i[n+1, k]|^2 \right\} \quad (14)$$

where $\bar{S}^i[n, k]$ is normalised to the maximum spectrogram value

$$\bar{S}^i[n, k] = \frac{S[n, k]}{\max_{n \in [0, N-1]; k \in [a_i, b_i]} S[n, k]}. \quad (15)$$

And lastly, we include fractal dimension as a spectral feature because of its relation to spectral shape [43]. We present two methods to estimate fractal dimension [43, 44]. The first method, proposed by Higuchi [43] and set with parameter `feat_params_st.fd.method='higuchi'`, generates an estimate of curve length $C_m(q)$ at different scale values q ,

$$C_m(q) = \frac{(N-1)}{\lfloor (N-m)/q \rfloor q^2} \sum_{i=1}^{\lfloor (N-m)/q \rfloor} |x[m+iq] - x[m+(i-1)q]|. \quad (16)$$

At each scale q , $C_m(q)$ is estimated over $m = 1, 2, \dots, q$ and then summarised by the mean value $C(q) = 1/q \sum_{m=1}^q C_m(q)$. For a self-similar and stationary process, $C(q) \propto q^{-D}$ where D is the fractal dimension [43]. By fitting a line to the points $(\log q, \log C(q))$ over $1 \leq q \leq q_{\text{max}}$, we estimate $-D$ as the slope of this line. To enforce an approximate linear sampling of $\log q$, scale values q are set to $q = 1, 2, 3, 4$ for $q \leq 4$ and $q = \lfloor 2^{(b+5)/4} \rfloor$ for $b = 5, 6, 7, \dots$ otherwise. The maximum value for q is set in parameter `feat_params_st.fd.qmax` and defaults to $q_{\text{max}} = 6$.

The second method, proposed by Katz and set with parameter `feat_params_st.fd.method='katz'`, is defined as follows [44]:

$$D = \frac{\log(N-1)}{\log(d/l) + \log(N-1)}. \quad (17)$$

Length l is defined as the sum of the Euclidean distance between consecutive points $(n, x[n])$ and $(n+1, x[n+1])$ as

$$l = \sum_{n=0}^{N-2} \sqrt{1 + (x[n+1] - x[n])^2} \quad (18)$$

Extent d is defined as the maximum (Euclidean) distance from starting point $(0, x[0])$ to any other point $(n, x[n])$ as

$$d = \max_{0 \leq n \leq N-1} \sqrt{n^2 + (x[n] - x[0])^2} \quad (19)$$

Note that (18) and (19) differ to the definition in the often-cited interpretation by Esteller *et al.* [45] which defines the distance measure on the 1-dimensional $x[n]$ and not on the 2-dimensional $(n, x[n])$ as originally intended [44].

4.3. Connectivity

We implement the brain symmetry index (BSI), which measures symmetry between hemispheres, according to the specifications in [46]. First, we estimate the PSD $P_m[k]$ for the m th channel of the EEG $x_m[n]$, for $m = 1, 2, \dots, M$. For $P_m[k]$, we can use either the periodogram in (5), the Welch periodogram in (6), or the robust-PSD estimate in (7), by setting the parameter `feat_params_st.connectivity.method` to either `'periodogram'`, `'PSD'` (default), or `'robust-PSD'`. Left-hemisphere channels are ordered from $m = 1, 2, \dots, M/2$ and right-hemisphere channels ordered for $m = M/2 + 1, M/2 + 2, \dots, M$. Next, we generate two PSDs as the mean PSD over all channels for each hemisphere; for example, for the left hemisphere,

$$P_{\text{left}}[k] = \frac{1}{M/2} \sum_{m=1}^{M/2} P_m[k]$$

where $P_m[k]$ represents the PSD estimate for the m th channel. A similar process produces $P_{\text{right}}[k]$ for the right channels. The symmetry measure quantifies the differences in two PSDs for the i th frequency band

$$C_{\text{BSI}}^i = \frac{1}{L_i} \sum_{k=a_i}^{b_i} \left| \frac{P_{\text{left}}[k] - P_{\text{right}}[k]}{P_{\text{left}}[k] + P_{\text{right}}[k]} \right| \quad (20)$$

where $[a_i, b_i]$ is the frequency range for the i th band and $L_i = b_i - a_i$.

Another measure of hemisphere connectivity correlates the signal envelope $e_i[n]$ in (1) for the i th frequency band between channels and across the hemispheres. Channels are grouped into pairs based on their regional location; for example, frontal channels are paired as $(F3, F4)$, central channels as $(C3, C4)$, and so on. Correlation coefficients (Pearson) are calculated for the m th pair $c_i(m)$, for $m = 1, 2, \dots, M/2$. The median is used to summarise over all pairs:

$$C_{\text{corr}}^i = \text{median}[c_i(m)]. \quad (21)$$

A global coherence measure is another approach to quantifying connectivity between regions across hemispheres. Coherence is calculated between channel pairs $x[n]$ and $y[n]$ as

$$C_{xy}[k] = \frac{|S_{xy}[k]|^2}{P_{xx}[k]P_{yy}[k]} \quad (22)$$

where $P_{xx}[k]$ (and $P_{yy}[k]$) is the auto PSD of $x[n]$ (and $y[n]$) using either the Welch periodogram in (6) or the robust-PSD in (7). The cross-PSD for $x[n]$ and $y[n]$, is calculated as

$$S_{xy}[k] = \frac{1}{LMU f_s} \sum_{l=0}^{L-1} \left(\sum_{n=0}^{M-1} x[n]w[n-lK]e^{-j2\pi kn/M} \sum_{n'=0}^{M-1} y[n']w[n'-lK]e^{j2\pi kn'/M} \right). \quad (23)$$

for the cross-Welch periodogram. The equivalent cross robust-PSD version replaces the mean operation over l , that is $1/L \sum_{l=0}^{L-1}$, with the median operator. Both the auto and cross PSDs estimates are set using the parameter `feat_params_st.connectivity.method='PSD'` (default) or `feat_params_st.connectivity.method='robust-PSD'`. Here, we assume that $y[n]$ and $w[n]$ are real-valued functions. Three features are used to summarise the coherence function $C_{xy}[k]$:

$$C_{\text{coh_mean}}^i = \frac{1}{L_i} \sum_{k=a_i}^{b_i} C_{xy}[k] \quad (24)$$

$$C_{\text{coh_max}}^i = \max_{k \in [a_i, b_i]} C_{xy}[k] \quad (25)$$

$$C_{\text{coh_freq_max}}^i = \operatorname{argmax}_{k \in [a_i, b_i]} C_{xy}[k] \quad (26)$$

Similar to correlation in (21), coherence features are estimated between the m th channel pairs and then summarised by the median value over all channel pairs.

To eliminate spurious coupling caused by inaccuracies in the coherence measure, we have implemented a null-hypothesis testing process to better estimate zero coherence [47, 48]. This approach generates a lower threshold by assessing the likelihood that a coherence measure represents either zero coherence (the null hypothesis) or non-zero coherence. An empirical probability distribution is generated from multiple uncoupled signals and is used to represent the null hypothesis that coherence is due to chance and not significantly different to zero. Here, we use the Fourier-transform shuffling method to generate these uncoupled, surrogate signals [47, 48]. The procedure, with a slight modification, is as follows:

1. compute the surrogate signal $u[n]$ for $x[n]$ (of length- N) as follows:
 - (a) generate length- N random phase $\varphi[k]$ from a uniform distribution in the range $[-\pi, \pi]$; enforce conjugate symmetry on $\varphi[k]$ with $\varphi[0] = 0$ and, if N is even, $\varphi[N/2] = 0$;
 - (b) multiply the magnitude spectrum of $x[n]$ by the random phase and Fourier transform back to the time domain

$$u[n] = \frac{1}{N} \sum_{k=0}^{N-1} |X[k]| e^{j\varphi[k]} e^{j2\pi kn/N};$$

2. generate $v[n]$ from $y[n]$ using a similar process;
3. estimate the coherence function for $u[n]$ and $v[n]$

$$C_{uv}[k] = \frac{|S_{uv}[k]|^2}{P_{xx}[k]P_{yy}[k]} \quad (27)$$

similar to (22) but using $P_{xx}[k]$ and $P_{yy}[k]$ from signals $x[n]$ and $y[n]$;

4. iterate this process N_{iter} times to generate the matrix $\mathbf{C}_{uv}[k]$ of dimension $N_{\text{iter}} \times N$;
5. let $T_{\text{lower}}[k]$ equal the $100(1 - \alpha)$ th percentile of $\mathbf{C}_{uv}[k]$ for each value of k , to determine if $C_{xy}[k]$ is statistical significant for $p < \alpha$;
6. generate coherence $C_{xy}[k]$ between $x[n]$ and $y[n]$ and threshold: set $C_{xy}[k] = 0$ for $C_{xy}[k] < T_{\text{lower}}[k]$.

Parameters N_{iter} and α are set by `feat_params_st.connectivity.coherence_surr_data` (default 100) and `feat_params_st.connectivity.coherence_surr_alpha` (default 0.05). To calculate coherence without this zero-coherence estimation procedure, set `feat_params_st.connectivity.coherence_surr_data=0`. The modification of the method here, not in the original procedure [47, 48], is to use $P_{xx}[k]$ instead of $P_{uu}[k]$ in (27). We base this on the assumption that because the magnitude spectrum for $u[k]$ and $x[k]$ are equal, therefore PSDs should also be equal. The whole procedure to generate the threshold $T_{\text{lower}}[k]$ can be slow and this modification reduces computational time by approximately one-half.

For all connectivity measures using the PSD, the window type and overlap for the PSDs can be set using the parameters `feat_params_st.connectivity.PSD_window` and `feat_params_st.connectivity.overlap`.

4.4. Burst and Inter-burst Intervals

The EEG of preterm infants shows a discontinuous pattern with short-duration bursts of activity alternating with longer quiescent periods. As the infant matures, the burst periods become longer and quiescent periods shorter so that eventually the EEG becomes continuous as the infant approaches term age. Discontinuous activity, which predominates in prematurity, consists of intermittent bursts against a background pattern of low-amplitude activity known as inter-burst intervals (IBI). To quantify this burst-inter-burst pattern, a burst detection method is needed to first detect the bursts before summarising the bursting pattern. We use the burst-detection algorithm proposed by O' Toole et al. [49]. The algorithm is freely available at https://github.com/otoolej/burst_detector and is used to generate the following features.

The burst detection algorithm estimates the burst annotation $b[n]$, with $b[n] = 0$ for inter-bursts and $b[n] = 1$ for bursts. Summary measures of temporal evolution of the bursting pattern include burst percentage, calculated as

$$B_{\text{burst}\%} = \frac{100}{N} \sum_{n=0}^{N-1} b[n] \quad (28)$$

and burst number $B_{\text{burst}\#}$, defined as the number of detected bursts over $b[n]$. Similarly, summary measures of the inter-burst pattern includes $B_{\text{IBI}_{\text{max}}}$, the maximum duration of all IBIs, and $B_{\text{IBI}_{\text{median}}}$ the median duration of IBIs.

4.5. Short-time and multi-channel analysis

Amplitude, frequency, and connectivity features are estimated on a short-time basis: features are calculated over a short duration window and this window is shifted in time; default window length is 64 seconds with an overlap of 50%, set with parameters `EPOCH_LENGTH` and `EPOCH_OVERLAP`. The median value is used to summarise these features over all analysis windows. For the amplitude, frequency, and bursting features, the features are estimated separately on each channel. Again, the median value is used to summarise over all channels.

5. Examples

5.1. Removing artefacts

To describe how the artefact removal procedure works, we present an example with simulated EEG. The function `gen_test_EEGdata.m` generates coloured Gaussian noise as a proxy for neonatal EEG:

```
1 % generates 2 minutes of EEG-like data sampled at 256 Hz:
2 Fs = 256;
3 data_st = gen_test_EEGdata(2*60,Fs,1);
```

The function returns the test data as both 9-channel referential montage (`data_st.eeg_data_ref`) and the 8-channel bipolar montage (`data_st.eeg_dat`). Next, we simulate a faulty recording on electrode F3:

```
1 N = size(data_st.eeg_data_ref,2);
2 if3 = find(strcmp(data_st.ch_labels_ref,'F3'));
3 data_st.eeg_data_ref(if3,:) = randn(1,N).*10;
```

Then simulate an electrode coupling between C4 and Cz

```
1 ic4 = find(strcmp(data_st.ch_labels_ref,'C4'));
2 icz = find(strcmp(data_st.ch_labels_ref,'Cz'));
3 data_st.eeg_data_ref(icz,:) = data_st.eeg_data_ref(ic4,:)+randn(1,N).*5;
```

and then re-generate the bipolar montage

```
1 [data_st.eeg_data,data_st.ch_labels] = set_bi_montage(...
2     data_st.eeg_data_ref,data_st.ch_labels_ref,data_st.ch_labels_bi);
```

The simulated EEG is displayed in Fig. 1 using the referential montage and in Fig. 2 using the bipolar montage.

To detect and remove these simulated artefacts, we use the `remove_artefacts.m` function:

```
1 eeg_art = remove_artefacts(data_st.eeg_data,data_st.ch_labels,...
2     data_st.Fs,data_st.eeg_data_ref,data_st.ch_labels_ref);
```

which returns the data in bipolar montage with channels C4-Cz and F3-C3 replaced by NaN values to indicate artefacts. The artefact identification process, relating to steps 1 and 2 in Section 3, is illustrated in Figs. 1 and 2.

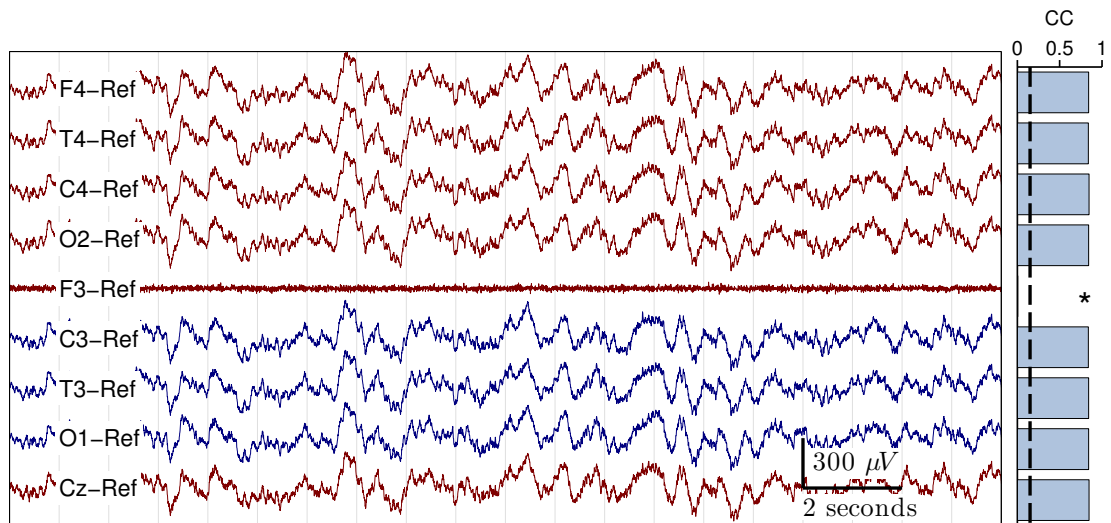


Figure 1: Referential montage of simulated EEG data (coloured Gaussian noise). All channels, except for F3, are highly correlated [correlation coefficient (CC) $r > 0.8$, right-hand side]. CCs are generated by averaging correlations between each channel and all other channels. Channels with CCs below the given threshold ($r = 0.15$, vertical dashed line) are removed (denoted with the * symbol), as is the case here for F3.

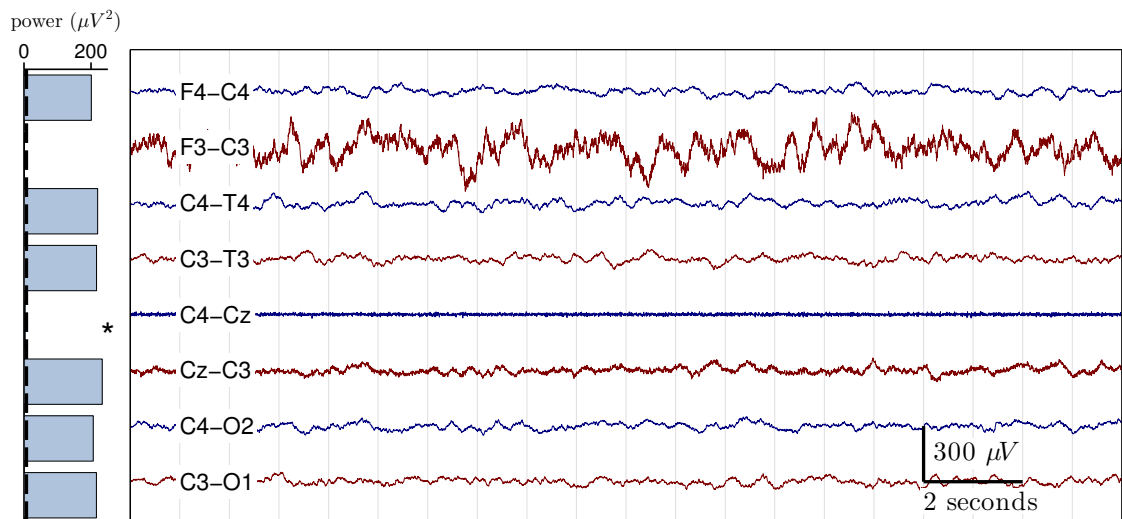


Figure 2: Bipolar montage of EEG in Fig. 1. Total power is assessed for each channel and plotted in left-hand side figure; channel F3-C3 is not included because F3 was removed in previous process (see Fig. 1). Channels with total power less than threshold (determined from median values of left and right hemisphere's separately) are denoted with * and removed from further analysis.

5.2. Calculating Features

Features are estimated using the `generate_all_features` function, as the following example shows. First, we generate 5 minutes of test data with a 64 Hz sampling rate:

```
1 data_st = gen_test_EEGdata(5*60,64,1);
```

Then, define the feature set as follows:

```
1 feature_set = {'spectral_relative_power', 'connectivity_BSI', 'rEEG_SD'};
```

Relative spectral power S_{relpow}^i and BSI C_{BSI}^i are defined in equations (9) and (20), respectively; standard deviation of rEEG R_{sd}^i is defined in Section 4.1. We can also use the parameter file `neural_parameters.m` to define the feature set. The full list of features are in Tables B.2–B.4. And lastly, we estimate the features using `generate_all_features`:

```
1 feat_st = generate_all_features(data_st, [], feature_set);
```

Features are returned as a structure, with 1 feature for each of the 4 frequency bands.

```
1 feat_st =
2     spectral_relative_power: [0.8672 0.0913 0.0350 0.0243]
3         connectivity_BSI: [0.0614 0.0489 0.0455 0.0505]
4             rEEG_SD: [3.1808 6.9492 4.5940 3.3538]
```

For the next example we calculate features of the rEEG. Simulated EEG, intended to resemble a discontinuous trace of preterm EEG, is generated as

```
1 data_st = gen_test_EEGdata(duration,Fs,1,1);
```

with `duration=4*60*60` (4 hours of EEG) and `Fs=64`. We then band-pass filter this simulated EEG with a 1–20 Hz filter by setting

```
1 feat_params_st.rEEG.freq_bands = [1 20];
```

in the parameter file (`neural_parameters.m`). Fig. 3(B) shows a 20-second epoch of the 4-hour multichannel EEG. We can view the rEEG by plotting the second output argument from the `rEEG` function

```
1 [~,reeg_left] = rEEG(data_st.eeg_data(7,:),Fs);
2 [~,reeg_right] = rEEG(data_st.eeg_data(8,:),Fs);
```

where `reeg_left` and `reeg_right` represent the rEEG generated for channels F3-C3 and F4-C4. These signals are plotted in Fig. 3(A). Next, assuming we want to estimate median, upper- and lower-margins of rEEG (R_{median} , R_{lower} , and R_{upper} as defined in Section 4.1), we do as follows:

```
1 feats = generate_all_features(data_st,{'F3-C3','F4-C4'}, ...
2     {'rEEG_lower_margin','rEEG_upper_margin','rEEG_median'});
```

For the example in Fig. 3, we find median value of $R_{\text{median}} = 228\mu V$, and lower–upper margins of [15–578] μV .

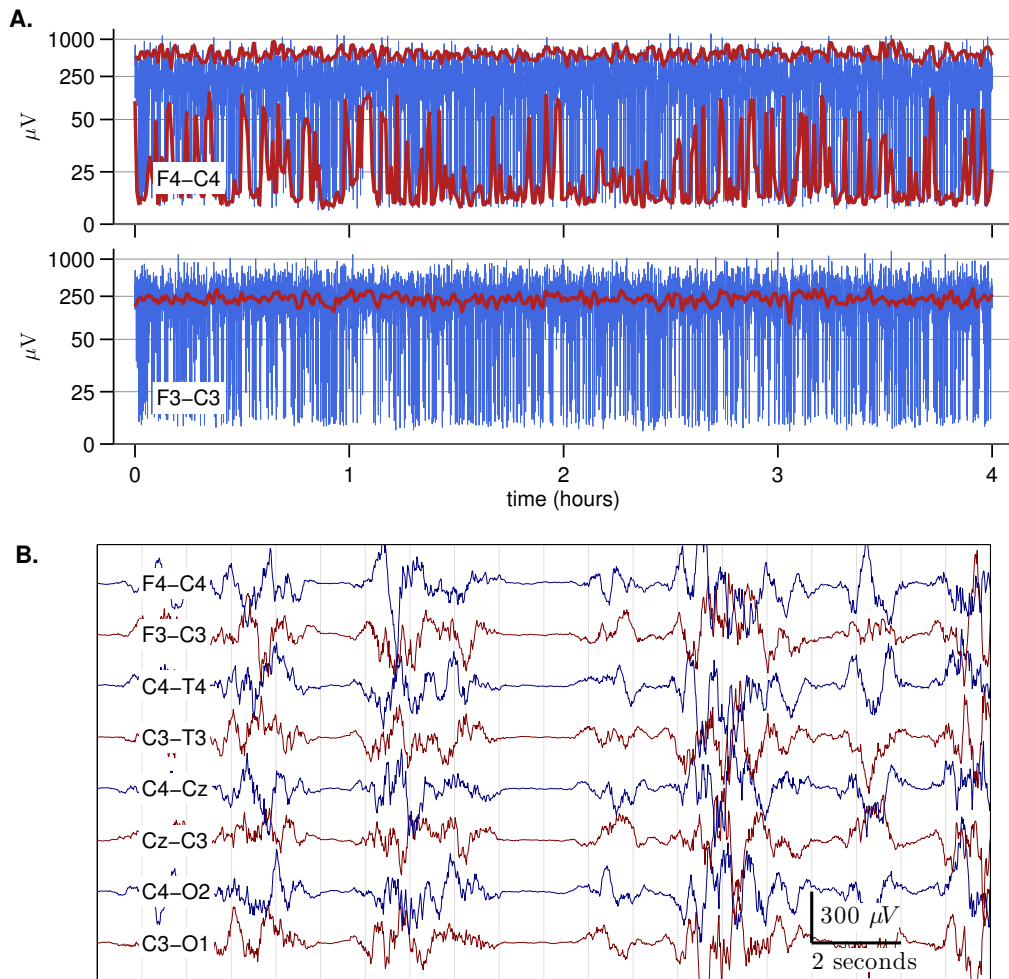


Figure 3: Estimating features with range-EEG (rEEG) using simulated EEG. A: 2-channels of rEEG (blue lines) over a 4-hour period. Red lines in top (A) represent upper- and lower-margins and median in bottom (A). B: 20 seconds of simulated preterm EEG.

6. Discussion

The presented feature set contains commonly-used features for quantitative analysis of newborn EEG. The set is implement in Matlab and freely available as open source code to use and modify as required [37]. The features are clearly defined with all implementation details. Research publications often omit these details yet they are essential for reproducible research and for comparing results across independent studies. For example, power in the delta frequency band will depend on a number of factors—such as filtering (if applied, and if so what type of filter used), power spectral density estimation (what type of estimate and what parameters used), and how to calculate the power (either sum over range in the frequency domain or energy of filtered signal in the time domain). Different implementations will give different estimates of the delta power, therefore undermining comparisons across studies. The availability of a common feature set, such as the one presented here, will enable both direct comparisons and reproducible research.

Our goal was to present quantitative features commonly used in newborn EEG [3, 14–36] and not include an exhaustive list of all possible features. For example, we restricted the set to stationary features and implemented a short-time procedure to accommodate for the non-stationary aspects of EEG. Although non-stationary methods have been used to analyse newborn EEG [11, 50–52], we do not include these here because of the following: first, these nonstationary methods are often developed for specific applications, such as detecting seizures [50]; second, their complexity limits their use, as typically a detailed-level of understanding of these methods is required before implementation [52]; and third, in many cases the assumption of short-time stationarity may be acceptable for the required application, for example in seizure detection [13]. Future iterations could expand the scope of feature set, to include features such as more advanced connectivity measures [53] or methods to quantify activity cycling in preterm newborns [54].

In conclusion, the NEURAL software package provides a common platform for quantitative analysis of multi-channel EEG for newborn infants. The software will assist reproducible research and consistency across independent studies. Many of the features, with the exception of the burst and inter-burst features, may also be of use for paediatric and adult EEG. These quantitative features can also be used to develop automated methods for newborn, such as automated detection of seizures [13, 50] or estimation of brain maturation [14].

7. Acknowledgements

This work was supported by Science Foundation Ireland (research-centre award INFANT-12/RC/2272 and investigator award 15/SIRG/3580). We thank Brian Murphy for help with testing the Matlab code.

Appendix A. Moments for Stationary Random Variable

The first 4 moments (mean, standard deviation, skewness, and kurtosis) for random variable $x[n]$ are estimated as follows: mean

$$\bar{x} = \frac{1}{N} \sum_{n=0}^{N-1} x[n],$$

standard deviation

$$s = \sqrt{\frac{1}{N-1} \sum_{n=0}^{N-1} |x[n] - \bar{x}|^2},$$

skewness

$$m_3 = \frac{\frac{1}{N} \sum_{n=0}^{N-1} |x[n] - \bar{x}|^3}{s^3},$$

and kurtosis

$$m_4 = \frac{\frac{1}{N} \sum_{n=0}^{N-1} |x[n] - \bar{x}|^4}{s^4}.$$

Appendix B. List of Features

Table B.1: Amplitude features with Matlab code name. Features are calculated for each frequency band.

name	description
amplitude_total_power	time-domain signal: total power
amplitude_SD	time-domain signal: standard deviation
amplitude_skew	time-domain signal: skewness
amplitude_kurtosis	time-domain signal: kurtosis
amplitude_env_mean	envelope: mean value
amplitude_env_SD	envelope: standard deviation
rEEG_mean	range EEG: mean
rEEG_median	range EEG: median
rEEG_lower_margin	range EEG: lower margin (5th percentile)
rEEG_upper_margin	range EEG: upper margin (95th percentile)
rEEG_width	range EEG: upper margin - lower margin
rEEG_SD	range EEG: standard deviation
rEEG_CV	range EEG: coefficient of variation
rEEG_asymmetry	range EEG: measure of skew about median

Table B.2: Spectral features with Matlab code name.

name	description
spectral_power [†]	spectral power: absolute
spectral_relative_power [†]	spectral power: relative (normalised to total spectral power)
spectral_flatness [†]	spectral entropy: Wiener (measure of spectral flatness)
spectral_entropy [†]	spectral entropy: Shannon
spectral_diff [†]	difference between consecutive short-time spectral estimates
spectral_edge_frequency	spectral edge frequency: 95% of spectral power contained between 0.5 and f_c Hz (cut-off frequency)
FD [†]	fractal dimension

[†] feature is calculated for each frequency band.

Table B.3: Connectivity features with Matlab code name. Features are calculated for each frequency band.

name	description
connectivity_BSI	brain symmetry index
connectivity_corr	correlation (Pearson) between envelopes of hemisphere-paired channels
connectivity_coh_mean	coherence: mean value
connectivity_coh_max	coherence: maximum value
connectivity_coh_freqmax	coherence: frequency of maximum value

Table B.4: Inter-burst interval features with Matlab code name.

name	description
IBI_length_max	burst annotation: maximum (95th percentile) inter-burst interval
IBI_length_median	burst annotation: median inter-burst interval
IBI_burst_prc	burst annotation: burst percentage
IBI_burst_number	burst annotation: number of bursts

References

- [1] Boylan GB, Stevenson NJ, Vanhatalo S. Monitoring neonatal seizures. *Seminars in Fetal & Neonatal Medicine*, 2013; 18(4):202–208.
- [2] André M, Lamblin MD, d’Allest AM, Curzi-Dascalova L, Moussalli-Salefranque F, Nguyen The Tich S, Vecchierini-Blieau MF, Wallois F, Walls-Esquivel E, Plouin P. Electroencephalography in premature and full-term infants. *Developmental features and glossary. Neurophysiol Clin*, 2010;40(2):59–124.
- [3] Lloyd RO, O’Toole JM, Livingstone V, Hutch WD, Pavlidis E, Cronin AM, Dempsey EM, Filan PM, Boylan GB. Predicting 2-y outcome in preterm infants using early multimodal physiological monitoring. *Pediatr Res*, 2016;80:382–388.
- [4] Boylan GB. Principles of EEG. In *Neonatal Cerebral Investigation*, chapter 2, 9–21. Cambridge University Press, 2008.
- [5] Tao JD, Mathur AM. Using amplitude-integrated EEG in neonatal intensive care. *J Perinatol*, 2010;30(S1):S73–S81.
- [6] Hagmann CF, Robertson NJ, Azzopardi D. Artifacts on electroencephalograms may influence the amplitude-integrated EEG classification: a qualitative analysis in neonatal encephalopathy. *Pediatrics*, 2006;118(6):2552–2554.
- [7] Suk D, Krauss AN, Engel M, Perlman JM. Amplitude-integrated electroencephalography in the NICU: frequent artifacts in premature infants may limit its utility as a monitoring device. *Pediatrics*, 2009;123(2):e328–332.
- [8] Marics G, Csek A, Vásárhelyi B, Zakariás D, Schuster G, Szabó M. Prevalence and etiology of false normal aEEG recordings in neonatal hypoxic-ischaemic encephalopathy. *BMC Pediatr*, 2013;13(1):194.
- [9] Stevenson NJ, Clancy RR, Vanhatalo S, Rosén I, Rennie JM, Boylan GB. Interobserver agreement for neonatal seizure detection using multichannel EEG. *Ann Clin Transl Neurol*, 2015;2(11):1002–1011.
- [10] Tokariev A, Palmu K, Lano A, Metsäranta M, Vanhatalo S. Phase synchrony in the early preterm EEG: development of methods for estimating synchrony in both oscillations and events. *Neuroimage*, 2012;60(2):1562–1573.
- [11] Omidvarnia A, Azemi G, Boashash B, O’Toole J, Colditz P, Vanhatalo S. Measuring time-varying information flow for scalp EEG signals: orthogonalized partial directed coherence. *IEEE Trans Biomed Eng*, 2014;61(3):680–693.
- [12] Greene BR, Faul S, Marnane WP, Lightbody G, Korotchkova I, Boylan GB. A comparison of quantitative EEG features for neonatal seizure detection. *Clin Neurophysiol*, 2008;119(6):1248–1261.
- [13] Temko A, Thomas E, Marnane W, Lightbody G, Boylan G. EEG-based neonatal seizure detection with support vector machines. *Clin Neurophysiol*, 2011;122(3):464–473.
- [14] O’Toole JM, Boylan GB, Vanhatalo S, Stevenson NJ. Estimating functional brain maturity in very and extremely preterm neonates using automated analysis of the electroencephalogram. *Clin Neurophysiol*, 2016;127(8):2910–2918.
- [15] Scher MS, Sun M, Steppe DA, Banks DL, Guthrie RD, Scwabassi RJ. Comparisons of EEG sleep state-specific spectral values between healthy full-term and preterm infants at comparable postconceptional ages. *Sleep*, 1994;17(1):47–51.
- [16] Duffy FH, Als H, McAnulty GB. Infant EEG spectral coherence data during quiet sleep: unrestricted principal components analysis—relation of factors to gestational age, medical risk, and neurobehavioral status. *Clin Electroencephalogr*, 2003; 34(2):54–69.
- [17] Paul K, Vladir K, Roth Z, Melichar J, Svojmil P. Comparison of quantitative EEG characteristics of quiet and active sleep in newborns. *Sleep Medicine*, 2003;4(6):543–552.
- [18] Scher MS. Automated EEG-sleep analyses and neonatal neurointensive care. *Sleep Medicine*, 2004;5(6):533–540.
- [19] West CR, Harding JE, Williams CE, Gunning MI, Battin MR. Quantitative electroencephalographic patterns in normal preterm infants over the first week after birth. *Early Hum Dev*, 2006;82(1):43–51.
- [20] Victor S, Appleton RE, Beirne M, Marson AG, Weindling AM. Spectral analysis of electroencephalography in premature newborn infants: normal ranges. *Pediatr Res*, 2005;57(3):336–341.

- [21] Pereda E, De La Cruz DM, Mañas S, Garrido JM, López S, González JJ. Topography of EEG complexity in human neonates: Effect of the postmenstrual age and the sleep state. *Neurosci Lett*, 2006;394(2):152–157.
- [22] Okumura A, Kubota T, Tsuji T, Kato T, Hayakawa F, Watanabe K. Amplitude spectral analysis of theta/alpha/beta waves in preterm infants. *Pediatr Neurol*, 2006;34(1):30–34.
- [23] Korotchikova I, Connolly S, Ryan CA, Murray DM, Temko A, Greene BR, Boylan GB. EEG in the healthy term newborn within 12 hours of birth. *Clin Neurophysiol*, 2009;120(6):1046–1053.
- [24] González JJ, Mañas S, De Vera L, Méndez LD, López S, Garrido JM, Pereda E. Assessment of electroencephalographic functional connectivity in term and preterm neonates. *Clin Neurophysiol*, 2011;122(4):696–702.
- [25] Thorngate L, Foreman SW, Thomas KA. Quantification of neonatal amplitude-integrated EEG patterns. *Early Hum Dev*, 2013;89(12):931–937.
- [26] Inder TE, Buckland L, Williams CE, Spencer C, Gunning MI, Darlow BA, Volpe JJ, Gluckman PD. Lowered electroencephalographic spectral edge frequency predicts the presence of cerebral white matter injury in premature infants. *Pediatrics*, 2003;111(1):27–33.
- [27] Korotchikova I, Stevenson NJ, Walsh BH, Murray DM, Boylan GB. Quantitative EEG analysis in neonatal hypoxic ischaemic encephalopathy. *Clin Neurophysiol*, 2011;122(8):1671–1678.
- [28] Williams IA, Tarullo AR, Grieve PG, Wilpers A, Vignola EF, Myers MM, Fifer WP. Fetal cerebrovascular resistance and neonatal EEG predict 18-month neurodevelopmental outcome in infants with congenital heart disease. *Ultrasound Obstet Gynecol*, 2012;40(3):304–309.
- [29] Saito M, Okumura A, Kidokoro H, Kubota T. Amplitude spectral analyses of disorganized patterns on electroencephalograms in preterm infants. *Brain Dev*, 2013;35(1):38–44.
- [30] Schumacher EM, Larsson PG, Sinding-Larsen C, Aronsen R, Lindeman R, Skjeldal OH, Stiris TA. Automated spectral EEG analyses of premature infants during the first three days of life correlated with developmental outcomes at 24 months. *Neonatology*, 2013;103(3):205–212.
- [31] Burdjalov VF, Baumgart S, Spitzer AR. Cerebral function monitoring: a new scoring system for the evaluation of brain maturation in neonates. *Pediatrics*, 2003;112(4):855–861.
- [32] Niemarkt HJ, Jennekens W, Pasman JW, Katgert T, Van Pul C, Gavilanes AWD, Kramer BW, Zimmermann LJ, Oetomo SB, Andriessen P. Maturation changes in automated EEG spectral power analysis in preterm infants. *Pediatr Res*, 2011; 70(5):529–534.
- [33] O’Reilly D, Navakatikyan MA, Filip M, Greene D, Van Marter LJ. Peak-to-peak amplitude in neonatal brain monitoring of premature infants. *Clin Neurophysiol*, 2012;123(11):2139–2153.
- [34] Meijer EJ, Hermans KHM, Zwanenburg A, Jennekens W, Niemarkt HJ, Cluitmans PJM, Pul CV, Wijn PFF. Functional connectivity in preterm infants derived from EEG coherence analysis. *Eur J Paediatr Neurol*, 2014;18(6):780–789.
- [35] Shany E, Meledin I, Gilat S, Yogev H, Golan A, Berger I. In and ex utero maturation of premature infants electroencephalographic indices. *Clin Neurophysiol*, 2014;125(2):270–276.
- [36] Saji R, Hirasawa K, Ito M, Kusuda S, Konishi Y, Taga G. Probability distributions of the electroencephalogram envelope of preterm infants. *Clin Neurophysiol*, 2015;126(6):1132–1140.
- [37] O’Toole JM. NEURAL: a neonatal EEG feature set in Matlab. GitHub Repository, 2016; ([online] https://github.com/otoolej/qEEG_feature_set).
- [38] Oppenheim AV, Schaffer RW. *Discrete-Time Signal Processing*. Prentice-Hall, Englewood Cliffs, NJ 07458, 1999.
- [39] Stevenson NJ, O’Toole JM, Korotchikova I, Boylan GB. Artefact detection in neonatal EEG. In *Int. Conf. IEEE Eng. Med. Biol. Soc. Chicago*, 2014;926–929.
- [40] Marple Jr SL. Computing the Discrete-Time “Analytic” Signal via FFT. *IEEE Trans Signal Process*, 1999;47(9):2600–2603.
- [41] Zhang D, Ding H. Calculation of compact amplitude-integrated EEG tracing and upper and lower margins using raw EEG data. *Health*, 2013;5:885–891.
- [42] Zoubir AM, Koivunen V, Chakhchoukh Y, Muma M. Robust estimation in signal processing: A tutorial-style treatment of fundamental concepts. *IEEE Signal Process Mag*, 2012;29(4):61–80.
- [43] Higuchi T. Approach to an irregular time series on the basis of the fractal theory. *Phys D: Nonlinear Phenom*, 1988; 31:277–283.
- [44] Katz MJ. Fractals and the analysis of waveforms. *Comput Biol Med*, 1988;18(3):145–156.
- [45] Esteller R, Echauz J, Tcheng T, Litt B, Pless B. Line length: an efficient feature for seizure onset detection. In *Int. Conf. IEEE Eng. Med. Biol. Soc.*, Istanbul, Turkey, 2001;1707–1710.
- [46] van Putten MJAM. The revised brain symmetry index. *Clin Neurophysiol*, 2007;118(11):2362–2367.
- [47] Prichard D, Theiler J. Generating surrogate data for time series with several simultaneously measured variables. *Phys Rev Lett*, 1994;73(7):951–954.
- [48] Faes L, Pinna GD, Porta A, Maestri R, Nollo G. Surrogate data analysis for assessing the significance of the coherence function. *IEEE Trans Biomed Eng*, 2004;51(7):1156–1166.
- [49] O’Toole JM, Boylan GB, Lloyd RO, Goulding RM, Vanhatalo S, Stevenson NJ. Detecting bursts in the EEG of very and extremely premature infants using a multi-feature approach. *Med Eng Phys*, 2017; DOI:10.1016/j.medengphy.2017.04.003
- [50] Stevenson NJ, O’Toole JM, Rankine LJ, Boylan GB, Boashash B. A nonparametric feature for neonatal EEG seizure detection based on a representation of pseudo-periodicity. *Med Eng Phys*, 2012;34(4):437–446.
- [51] Mesbah M, O’Toole JM, Colditz PB, Boashash B. Instantaneous frequency based newborn EEG seizure characterization. *EURASIP J Adv Signal Process*, 2012;2012(143).
- [52] Boashash B, Azemi G, O’Toole JM. Time–frequency processing of nonstationary signals: advanced TFD design to aid diagnosis with highlights from medical applications. *IEEE Signal Process Mag*, 2013;30(6):108–119.

- [53] Omidvarnia A, Fransson P, Metsäranta M, Vanhatalo S. Functional bimodality in the brain networks of preterm and term human newborns. *Cereb Cortex*, 2014;24(10):2657–2668.
- [54] Stevenson NJ, Palmu K, Wikström S, Hellström-Westas L, Vanhatalo S. Measuring brain activity cycling (BAC) in long term EEG monitoring of preterm babies. *Physiol Meas*, 2014;35(7):1493–1508.